DELAWARE RIVER BRIDGE FRACTURE: REPAIR STRATEGY AND MONITORING BY DIGITAL IMAGE CORRELATION

YAO WANG

ASHLEY P. THRALL

THEODORE P. ZOLI

BIOGRAPHY

Yao Wang is a Graduate Student in the Kinetic Structures Laboratory in the Department of Civil & Environmental Engineering & Earth Sciences at the University of Notre Dame. Prior to pursuing her PhD at Notre Dame, she earned her MS and BS degrees in Civil Engineering from Harbin Institute of Technology (HIT), China.

Dr. Ashley P. Thrall is the Myron and Rosemary Noble Associate Professor of Structural Engineering in the Department of Civil & Environmental Engineering & Earth Sciences at the University of Notre Dame where she directs the Kinetic Structures Laboratory. Dr. Thrall earned her PhD and MSE in Civil & Environmental Engineering from Princeton University and her BA in Physics from Vassar College.

Theodore P. Zoli, PE is the National Bridge Chief Engineer and a Senior Vice President at HNTB Corporation. He has served as a bridge designer for over 25 years, leading the design of many projects including the Leonard P. Zakim Bunker Hill Bridge in Boston, the Blennerhassett Island Bridge between West Virginia and Ohio, the Bob Kerrey Pedestrian Bridge between Nebraska and Iowa, the Lake Champlain Bridge between New York and Vermont, and the Memorial Bridge between New Hampshire and Maine. He earned his MS from the California Institute of Technology and his BS from Princeton University.

SUMMARY

The Delaware River Bridge, constructed in 1956 by American Bridge (owned by US Steel), is a continuous truss bridge that links the New Jersey Turnpike and Pennsylvania Turnpike. On January 20, 2017, a fracture in the upper chord of its four-span continuous approach was discovered and the bridge was subsequently closed to traffic.

The fracture occurred in a W14 x 314 rolled section in the upper chord of the North truss of the four-span continuous approach above the fixed bearing. The load redistributed to surrounding members, notably the neighboring upper chord W14 x 87 section which buckled about its weak axis. Both the North and South trusses vertically deflected. The bridge was repaired by (1) vertically jacking the structure from towers to restore the vertical position of the trusses, followed by (2) post-tensioning and splicing the fractured member to restore the original dead load force in that member. This paper will discuss the repair strategy and implementation which was monitored using Digital Image Correlation (DIC).

Throughout the repair process, the strain in the flanges of seven members was monitored using DIC. DIC is a non-destructive, photographic technique that can measure full-field, three-dimensional strains with high accuracy. This is the first time that DIC has been utilized to monitor a bridge during repairs. The paper will discuss this technology and present the measured strains from the post-tensioning repair process.

DELAWARE RIVER BRIDGE FRACTURE: REPAIR STRATEGY AND MONITORING BY DIGITAL IMAGE CORRELATION

Introduction

The Delaware River Bridge (Figures 1 and 2), constructed in 1956 by American Bridge (owned by US Steel), is a continuous truss bridge that links the New Jersey Turnpike and Pennsylvania Turnpike. On January 20, 2017, a fracture in the upper chord of its four-span continuous approach was discovered and the bridge was subsequently closed to traffic.

The fracture occurred in U19'-20 (where U indicates upper chord and the numbering refers to the nodes identified in Figure 2), a W14 x 314 rolled section with a design force of 1851 kips, in the upper chord of the North truss of the four-span continuous approach above the fixed bearing (Figures 1 and 2). The load redistributed to the surrounding members, notably the neighboring upper chord U18'-19', a W14 x 87 rolled section with design tension force of 364 kips and compressive force of 251 kips, which buckled about its weak axis. The fracture also caused the deformation of adjacent verticals and sway bracing. Further, both the North and South trusses vertically deflected (the North more than the South). The bridge was repaired by 1) vertically jacking the structure from towers to restore the vertical position of the trusses, followed by 2) post-tensioning and splicing the fractured member to restore the original dead load force in that member. Following this repair and live load testing, the bridge was successfully reopened to traffic on March 9, 2017.

Throughout the repair process, the behavior of seven members (Figures 1 and 2) was monitored using three-dimensional Digital Image Correlation (DIC). DIC is a non-contact, non-destructive photographic monitoring technique that measures full-field strains and displacements using pattern recognition and photogrammetric triangulation principles. Compared to traditional instrumentation - such as strain gauges or displacement transducers which measure discrete, fixed direction strain and displacement - DIC captures three-dimensional, full-field strain and displacement distributions. The direction of the strains can be selected in post-processing and strain gradients can also be obtained. For bridge monitoring, DIC provides additional advantages as it is portable and does not require wiring or an on-site data acquisition system (1).

This paper presents the repair strategy that was successfully implemented and discusses the behavior of three of the upper chord members (i.e., U17'-18', U18'-19', U20-19; see Figures 1 and 2) which were monitored via DIC during the process.

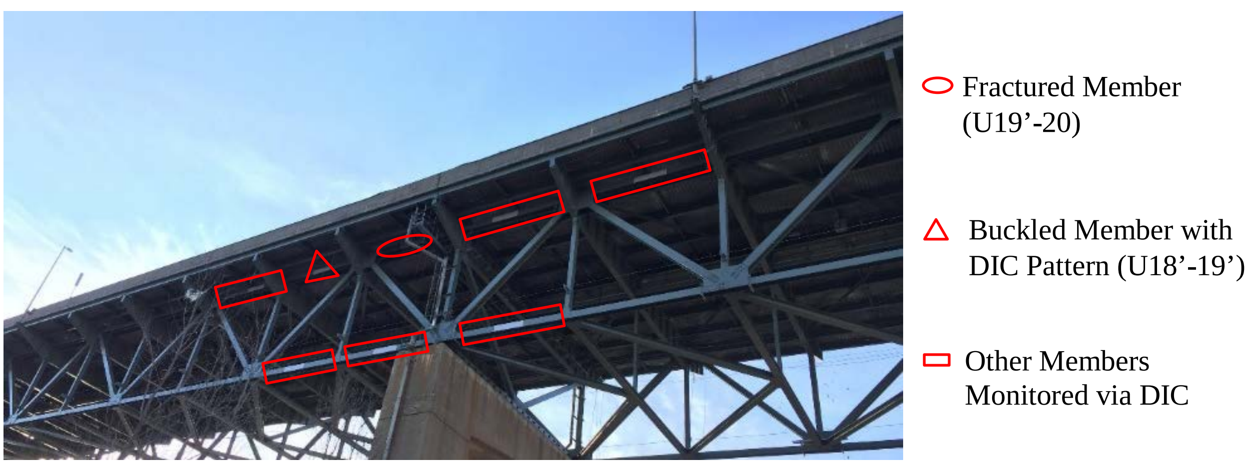

Figure 1 Photograph of the North truss of the Delaware River Bridge, highlighting the fractured and buckled members, as well as the members monitored by DIC.

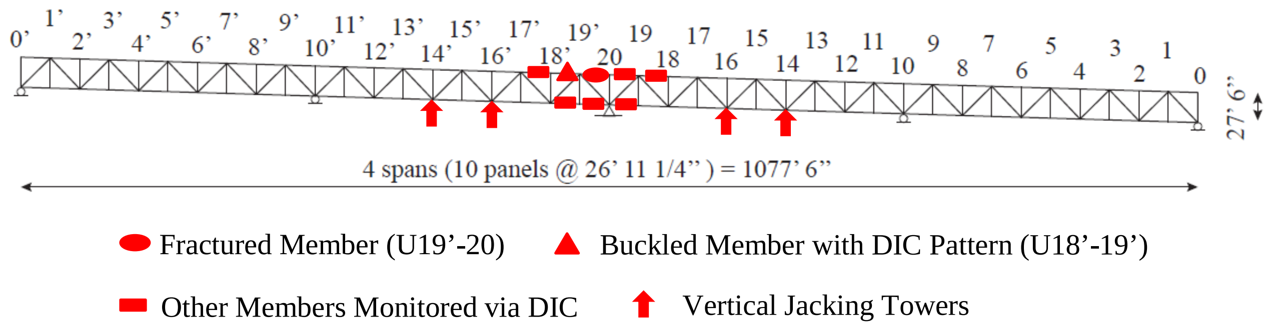

Figure 2 Elevation of the North truss, indicating node numbers and locations for jacking towers. The fractured and buckled members, as well as the members monitored by DIC, are highlighted.

Delaware River Bridge Repair

The fracture in U19'-20 was discovered on January 20, 2017. A temporary stabilization splice was immediately installed to re-connect the member. The repair was then performed in two stages: (1) vertical jacking and (2) post-tensioning.

The aim of the vertical jacking was to restore the vertical position of the trusses. The temporary splice was first removed. The jacking was performed from eight 80-ft high temporary towers that were erected for this purpose. Four towers were located under the South truss (located under nodes 14', 16', 16 and 14) and four were located under the North truss at symmetric locations (Figures 2 and 3). The pressure in the jacks under the trusses at nodes 16' and 16 were gradually increased in four phases: 25%, 50%, 75% and 100% of the repair design pressure. The other jacks remained in contact during this process. The entire procedure was completed on February 24, 2017.

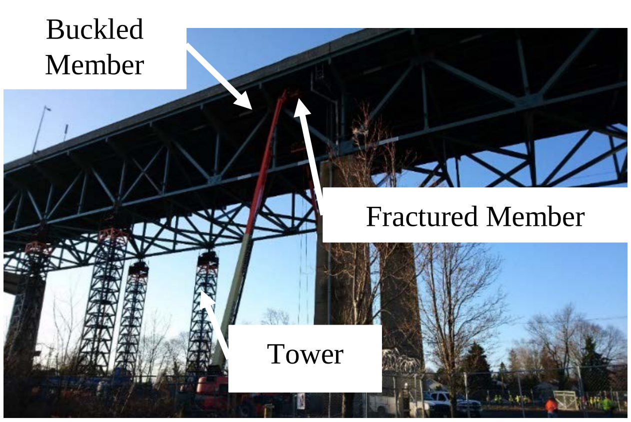

Figure 3 Photograph of vertical jacking towers.

Post-tensioning was then performed with the aim of restoring the original dead load force in the fractured member. First, the steel surrounding the fractured region was removed and replaced. Post-tensioning bars and brackets were installed (Figure 4). The bars were tensioned on March 3, 2017 in two phases: 90% and 100% of the post-tensioning design force of 1500 kips. A permanent splice was then installed on March 4, 2017 (Figure 4). Additional steel channel sections were added to reinforce the buckled member, U18'-19' with the aim of compensating for the Bauschinger effect (Figure 5). On March 5, the post-tensioning was released and the post-tensioning system was demobilized.

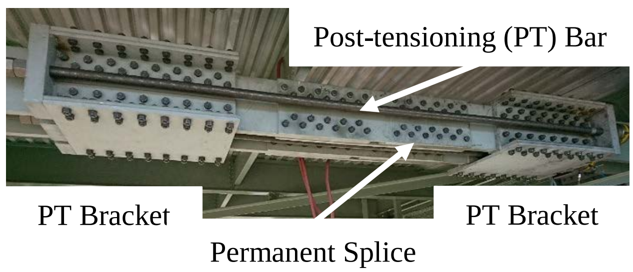

Figure 4 Photograph of post-tensioning system.

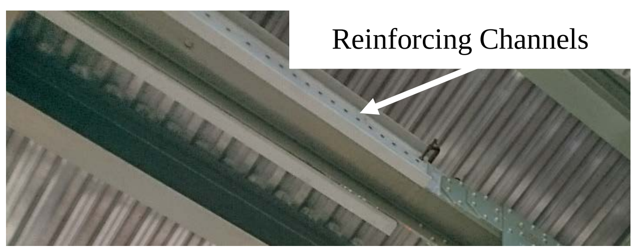

Figure 5 Photograph of reinforcing channels (during installation).

Live load tests, including four crawl tests (3 runs for each test), one speed test (3 runs), and seven static tests, were performed on March 7, 2017 to ensure that the repaired bridge could be reopened to the public safely. The bridge was ultimately reopened to traffic on March 9, 2017.

Experimental Program

The surface strains in seven members of the North truss (Figures 1 and 2) were measured via DIC. In three-dimensional DIC, photographs of specimens are taken before and after loading using two cameras mounted on a rigid bar. A pattern of random black and white lines or ellipses must first be applied to the specimen in the region of interest. A software package then calculates the three-dimensional strains and displacements using pattern recognition and photogrammetric triangulation principles.

DIC has previously been used to monitor many types of bridges, including steel girder bridges (2-7), suspension bridges (8), and bascule bridges (9). Due to its advantages over traditional instrumentation, DIC has been used to measure both static deformation and dynamic response of bridges. The measurements include displacements (2, 4-7, 9-11), cracks (12-13), frequencies (6, 8, 14), and strain distributions (3, 15). Most of this existing research focuses on monitoring vertical deflections since this can be used to determine the overall stiffness.

The DIC system used in this research featured two 2448 x 2050 pixel cameras with 12 mm lenses. The GOM Correlate (16) software package was used to perform the image correlation, calculating the strains. The pattern was applied to a 6-ft long region of the exterior flanges of the monitored members, approximately in the middle of the length of each member (Figure 6). The data in this paper focuses on the middle 3-ft length of the monitored region (i.e., the "Selected Data" region in Figure 6). It also neglects the extreme edges in the y-direction to avoid noise associated with image correlation at the edges of a pattern. All strains, ε in this paper are calculated using a gauge length of 1.27 in. The focus is on strains in the longitudinal or x-direction of the member identified in Figure 6 (i.e., along the axis of the member).

While the ideal accuracy of the strains measured by the GOM Correlate software package is 100 microstrain, additional noise can result from the complete hardware-software system and environmental effects. As reviewed in Wang et al. (1), noise can be reduced by area averaging (where strains are averaged over a region) and time averaging (where strains are averaged over multiple DIC frames taken within a short period of time). For the full-field strain maps in Figure 7, the median filter was applied for area averaging and the binomial filter was applied for time averaging in GOM Correlate (16). The quantified strain values, ε provided in the right column in Figure 7 use additional area averaging. This additional area averaging is performed over the "total" selected data area in Figure 6 for members U17'-18' and U20-19 where behavior is primarily axial. For U18'-19', where flexural behavior is observed, area averaging is performed for the "top," "middle," and "bottom" regions as identified in Figure 6.

For all data in this paper, strains are measured relative to DIC photographs taken on January 30, 2017 (hereafter referred to as reference frames), when the temporary stabilization splice was in place. These reference frames can also be used to indicate noise of the complete hardware-software system. The average value of strain from these reference frames is approximately zero. Two standard deviations from this average can be used as a measure of the noise, which is 120 microstrain in this research.

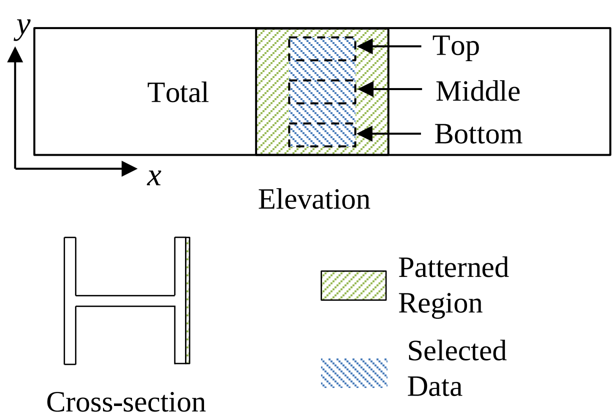

Figure 6 Sketch of a monitored truss member, indicating the patterned and selected data area.

Results

Although seven members were monitored during the vertical jacking and post-tensioning procedures, this paper focuses on the behavior of three upper chord members during post-tensioning: U17'-18', U18'-19' (i.e., the buckled member), and U20-19.

Monitoring was performed at 90% post-tensioning, 100% post-tensioning, post-tensioning release, and when the jacks on the vertical towers were released and were no longer in contact with the trusses (just prior to when live load tests were performed). Not all measurements could be made at each stage of repair due to challenges in timing, lighting, and also high winds. The pattern on U18'-19' was obscured due to the reinforcing channels (Figure 5), and so results could not be obtained after 100% post-tensioning.

Figure 7 shows the full-field measured strains in U17'-18', U18'-19', and U20-19, as well as the discrete values after area averaging. Some bands are observed in the measured strain distributions. This can be attributed to some flexural behavior, geometric imperfections of the members, inhomogeneity in the grain structure of the steel, and noise. During post-tensioning, tensile strains were introduced in all of the upper chords, as expected. From 90% to 100% post-tensioning, the magnitude of strain increased in each of the members, also as expected. Assuming a Young's Modulus of 29,000 ksi and using the known area of steel in the section, the axial force in U20-19 at 100% post-tensioning is 1581 kips based on the measured strain. This is very close to the post-tensioning design force of 1500 kips. As U20-19 theoretically (assuming truss behavior) has the same force as U19'-20 which is being post-tensioned, this magnitude of force is expected. The slight difference can be attributed to any out-of-plane bending that may have occurred. As the DIC measurements are made on the flange of the member, the results would be more susceptible to out-of-plane bending.

When post-tensioning was released, the tension in the members decreased significantly, particularly for U20-19. This can be attributed to the fact that the North truss might have settled back on the towers. During post-tensioning, the North truss was expected to fully lift off of the temporary towers. However, daylight was never observed for several of the jacks on the towers. U20-19 was also monitored on the day of the live load test, when the jacks were released and the North truss was no longer in contact with the temporary towers. DIC measurements taken when there was no load on the truss indicate that the tensile strains induced during post-tensioning are mostly restored when the truss was no longer in contact with the towers.

The post-tensioning operation was intended to relieve stress from member U18'-19'. Visually, it was observed that U18'-19' did not fully straighten under the post-tensioning operation. However, flexural strains (i.e., higher tensile strains on the top than the bottom) shown in Figure 7 do indicate unbending.

Conclusions

This paper presented the repair procedure of the Delaware River Bridge. The behavior of seven members during the repair was measured via DIC and results were reported for three of these members, focusing on the upper chord near the fracture. The measured strains match the post-tensioning force closely and the members behaved as expected.

Acknowledgements

This work was supported by the New Jersey Turnpike Authority. The work of Lee Bertolet, Jefferson Soica, and Vasili Trikoupis in operating the manlift during monitoring is greatly appreciated. The authors are grateful to Craig Sanford of Slicks Graphics for applying the DIC pattern at a reduced cost. The authors also appreciate the assistance of graduate students Evan J. Gerbo and Mirela D. Tumbeva.

Stage of Repair	Full-field Strain	Microstrain	
		Color Scale	Value
Member U17'-18':			
90% PT	NA	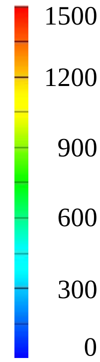	NA
100% PT	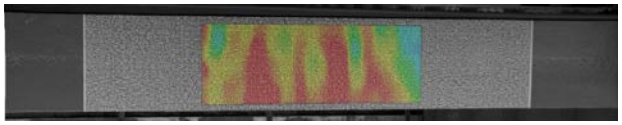		ε_{total} = 1180
PT Released	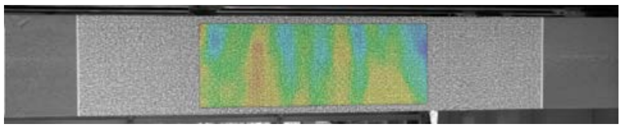		ε_{total} = 800
Member U18'-19':			
90% PT	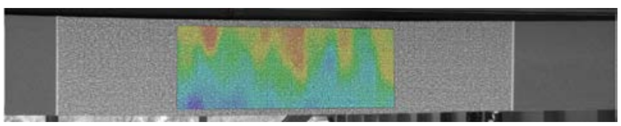	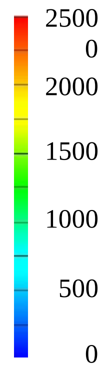	ε_{top} = 1770 ε_{middle} = 1220 ε_{bottom} = 640
100% PT	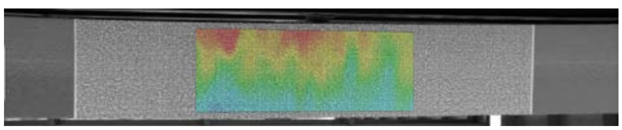		ε_{top} = 2080 ε_{middle} = 1460 ε_{bottom} = 800
PT Released	NA		NA
Member: U20-19:			
90% PT	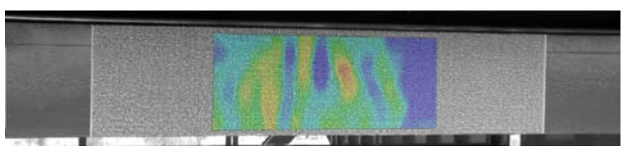	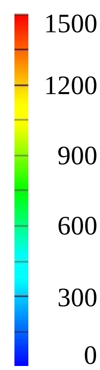	ε_{total} = 470
100% PT	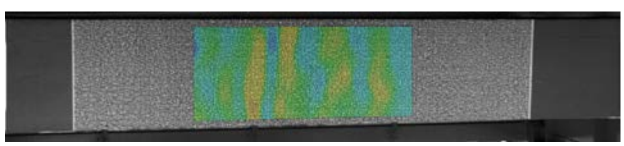		ε_{total} = 690
PT Released	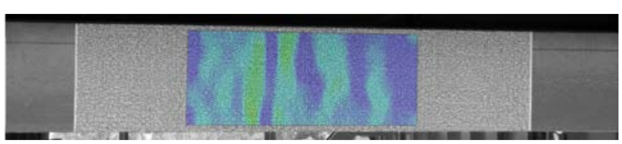		ε_{total} = 220
Tower Jacks Released	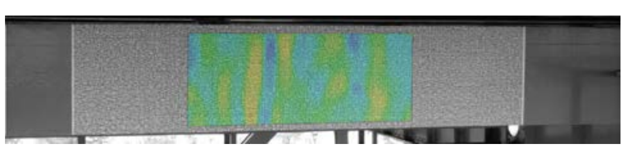		ε_{total} = 640

Figure 7 Strains in the longitudinal direction (x-direction, Figure 6) due to post-tensioning (PT). NA=Not Available.

References

1. Wang, Y., Tumbeva, M.D., Thrall, A.P. and Zoli, T.P. (2018). “Monitoring steel bridges via digital image correlation: pressure-activated adhesive pattern.” Journal of Bridge Engineering, In review.
2. Bell, E.S., Peddle, J.T. and Goudreau, A. (2012). “Bridge condition assessment using digital image correlation and structural modeling.” Proceedings of the Sixth International Conference on Bridge Maintenance, Safety and Management, 165(4), 330-337.
3. Winkler, J. and Hendy, C. (2017). “Improved structural health monitoring of London’s Docklands light railway bridges using digital image correlation.” Structural Engineering International, 27(3), 435-440.
4. Peddle, J., Goudreau, A., Carlson, E. and Santini-Bell, E. (2011). “Bridge displacement measurement through digital image correlation.” Bridge Structures, 7(4), 165-173.
5. Chiang, C.-H., Shih, M.-H., Chen, W. and Yu, C.-P. (2011). “Displacement measurements of highway bridges using digital image correlation methods.” Proceedings of the SPIE - The International Society for Optical Engineering, 8321.
6. Hoag, A.J., Hoult, N.A., Take, W.A. and Le, H. (2015) “Monitoring of rail bridge displacements using digital image correlation.” Proceedings of the 10th International Workshop on Structural Health Monitoring, 2, 399-406.
7. Yoneyama, S., Kitagawa, A., Iwata, S., Tani, K. and Kikuta, H. (2007). “Bridge deflection measurement using digital image correlation.” Experimental Techniques, 31(1), 34–40.
8. Kim, S.-W. and Kim, N.-S. (2013). “Dynamic characteristics of suspension bridge hanger using digital image correlation.” NDT-E International, 59, 25-33.
9. Hoag, A., Hoult, N. and Take, A. (2017). “Assessment of a bascule lift bridge using digital image correlation.” Proceedings of the ICE – Bridge Engineering, 170(BE3), 168-180.
10. DeRoover, C., Vantomme, J., Wastiels, J. and Taerwe, L. (2003). “DIC for deformation assessment: a case study.” European Journal Mech. and Env. Eng., 48(1), 13-19.
11. Pan, B., Tian, L. and Song, X. (2016). “Real-time, non-contact and targetless measurement of vertical deflection of bridges using off-axis digital image correlation.” NDT&E International, 79, 73-80.
12. Kuntz, M., Jolin, M., Bastien, J., Perez, F. and Hild, F. (2006). “Digital image correlation analysis of crack behavior in a reinforced concrete beam during a load test.” Can. J. Civ. Eng., 33, 1418-1425.
13. Baah, P. (2014). “Cracking behavior of structural slab bridge decks.” Ph.D. thesis, University of Akron, Akron, OH.
14. Busca, G., Cigada, A., Mazzoleni, P. and Zappa, E. (2014). “Vibration monitoring of multiple bridge points by means of a unique vision-based measuring system.” Experimental Mechanics, 54(2), 255–271.
15. Nonis, C., Niezrecki, C., Yu, T.-Y., Ahmed, S., Su, C.-F., and Schmidt, T. (2013). “Structural health monitoring of bridges using digital image correlation.” Proceedings of the SPIE – The International Society for Optical Engineering, 8695.
16. GOM Correlate (2013). “GOM Correlate 2017.” Braunschweig, Germany.